Nucleation of ethanol, propanol, butanol, and pentanol: A systematic experimental study along the homologous series

Alexandra A. Manka, Jan Wedekind, David Ghosh, Kristina Höhler, Judith Wölk et al.

Additional information on J. Chem. Phys.

Nucleation of ethanol, propanol, butanol, and pentanol: A systematic experimental study along the homologous series

Alexandra A. Manka,[1] Jan Wedekind,[2,a)] David Ghosh,[3] Kristina Höhler,[4] Judith Wölk,[1] and Reinhard Strey[1]

[1]*Institut für Physikalische Chemie, Universität zu Köln, Luxemburgerstr. 116, D-50939 Köln, Germany*
[2]*Departament de Física Fonamental, Universitat de Barcelona, Martí i Franquès 1, 08028 Barcelona, Spain*
[3]*Philip Morris International, Research Development, Quai Jeanrenaud 5, 2000 Neuchâtel, Switzerland*
[4]*Institute for Meteorology and Climate Research, Atmospheric Aerosol Research (IMK-AAF),*
Karlsruhe Institute of Technology (KIT), 76021 Karlsruhe, Germany

We present homogeneous vapor-liquid nucleation rates of the 1-alcohols ($C_nH_{2n+1}OH$, n = 2–4) measured in the well-established two-valve nucleation pulse chamber as well as in a novel one-piston nucleation pulse chamber at temperatures between 235 and 265 K. The nucleation rates and critical cluster sizes show a very systematic behavior with respect to the hydrocarbon chain length of the alcohol, just as their thermo-physical parameters such as surface tension, vapor pressure, and density would suggest. For all alcohols, except ethanol, predictions of classical nucleation theory lie several orders of magnitude below the experimental results and show a strong temperature-dependence typically found in nucleation experiments. The more recent *Reguera-Reiss* theory [J. Phys. Chem. B **108**(51), 19831 (2004)] achieves reasonably good predictions for 1-propanol, 1-butanol, and 1-pentanol, and independent of the temperature. Ethanol, however, clearly shows the influence of strong association between molecules even in the vapor phase. We also scaled all experimental results with classic nucleation theory to compare our data with other data from the literature. We find the same overall temperature trend for all measurement series together but inverted and inconsistent temperature trends for individual 1–propanol and 1–butanol measurements in other devices. Overall, our data establishe a comprehensive and reliable data set that forms an ideal basis for comparison with nucleation theory. © *2012 American Institute of Physics*. [http://dx.doi.org/10.1063/1.4739096]

I. INTRODUCTION

The first step in almost any first-order phase transitions is nucleation, i.e., the formation of the first initial fragments or clusters of the new phase out of the mother phase. These small clusters of only a few molecules form through density fluctuations in the mother phase and first need to overcome a free-energy barrier before they can serve as nuclei of the new phase. Homogeneous vapor-liquid nucleation, the formation of liquid droplets from condensable vapors in the absence of any foreign particles or surfaces, has been studied for over a hundred years.[1] Several different experimental devices and methods have been developed to investigate nucleation as a function of supersaturation and temperature.[2] These devices include supersonic nozzles,[3,4] shock tubes,[5] thermal diffusion cloud chambers,[6–8] laminar flow diffusion chambers,[9,10] and nucleation pulse chambers.[11,12] Each of these experiments cover different temperature and pressure ranges. Consequently, many orders of magnitude in the nucleation rate J, the number of nuclei formed per unit time and per unit volume, starting from $J = 10^{-3}$ cm^{-3} s^{-1} up to $J = 10^{18}$ cm^{-3} s^{-1}, are observed altogether.[13] At the same time, several nucleation theories have been developed, such as classical nucleation theory (CNT),[14–16] density functional

theory,[17] dynamic nucleation theory (DNT),[18] *Reguera-Reiss* theory (RRT),[19,20] based on a combination of the extended modified liquid drop model[21,22] and DNT, the mean-field kinetic nucleation theory,[23] and some more.[24,25] All these theories intend to describe and predict the nucleation behavior of any arbitrary substances. Nevertheless, despite tremendous efforts, huge deviations of up to some 20 orders of magnitude between these theories and experimental result can still be found.[26]

The 1-alcohols form one class of compounds with several advantages for the investigation of nucleation. They are accessible by most experiments, have experimentally convenient vapor pressures and because condensation occurs above their respective triple point, their physical properties such as the equilibrium vapor pressure, the surface tension, and the density are well known.[27–29] Furthermore, they allow a study along a homologous series, along which all physico-chemical parameters vary very systematically. Therefore, it is no surprise that the 1–alcohols have been the subject of many investigations in the past.[30–49]

Here we present the results of our measurements in the well-established two-valve nucleation pulse chamber (NPC) and in a novel one-piston expansion chamber (OPC). The measuring window for both devices is the same and with nucleation rates of $10^5 < J_{\mathrm{exp}}/$cm^{-3} s$^{-1} < 10^9$, located in the middle of the experimentally accessible nucleation rate regime. We have measured vapor-liquid nucleation rate isotherms of

a)Author to whom correspondence should be addressed. Electronic mail: janw@ffn.ub.es.

ethanol, 1–propanol, and 1-butanol in the NPC as well as of 1–butanol in the OPC using argon as carrier gas. We append our data with the 1–pentanol data from Iland *et al.*[13] measured also in the NPC. The data also include a comparison of different carrier gases, helium and argon. We compare all data to CNT as well as to RRT. Using the nucleation theorem,[50–52] the excess number of molecules in the critical clusters is determined as a function of temperature for each alcohol, respectively. These experimental critical cluster sizes are compared to cluster sizes predicted by the classical *Gibbs-Thomson* equation and by RRT. Finally, we reduce all experimental data from literature with classical nucleation theory to compare them with our data.

II. EXPERIMENTAL TECHNIQUE

The experimental setup and the measuring procedure of the NPC have already been described in detail by Strey *et al.*[12] Therefore, we just repeat the principles and fundamental issues here. The two-valve nucleation pulse chamber consists of three adjacent volumes, the expansion volume, the main measuring volume in the middle, and the recompression volume. All of them are separated by a valve while between the recompression volume and the main chamber volume an additional membrane is located.[12] A well-defined vapor-carrier-gas mixture is drawn to the main volume at a defined pressure p_0 while the pressure in the expansion volume is set to a value lower than p_0. The valve to the expansion volume opens and the mixture expands adiabatically to a lower pressure p_{exp} and, consequently, to a lower temperature T_{exp}. The vapor reaches the metastable state and the supersaturation S which is defined as the ratio of the actual vapor pressure p_v to the equilibrium vapor pressure p_{eq} of the condensable species at the given temperature T_{exp},

$$S = \omega \frac{p_{exp}}{p_{eq}(T_{exp})} = \frac{p_v}{p_{eq}(T_{exp})}, \quad (1)$$

where ω is the ratio of vapor pressure to the total pressure of the vapor and carrier-gas mixture, increases. Once the supersaturation exceeds a critical value S^*, nucleation sets in. After a short time of typically 1 ms the second valve to the recompression volume opens, the membrane separating the recompression volume from the main volume everts and the mixture gets slightly recompressed. Nucleation stops abruptly as the saturation ratio drops under the critical value but the vapor phase still remains saturated ($1 < S < S^*$). Thus, nucleation and growth are effectively decoupled. Only already formed nuclei are able to grow to microscopic droplets of optically detectable size.

The number density N of the formed droplets in the main volume is measured by constant-angle-Mie-scattering.[53] Due to the fact that nucleation and growth are decoupled, the nucleation time Δt is limited to the length of the plateau of the pressure pulse at p_{exp} before recompression. The nucleation rate can then be calculated via

$$J = \frac{N}{\Delta t}. \quad (2)$$
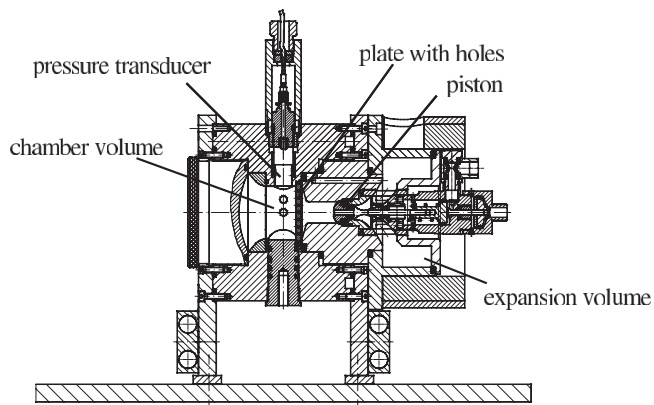
FIG. 1. Technical drawing of the one-piston expansion chamber. The expansion volume is located around the pulse-generating piston.

In addition to the measurements with the two-valve nucleation pulse chamber, we also conducted measurements with a novel one-piston expansion chamber (see Fig. 1). Therefore, we changed the setup of the central chamber but did not modify anything in the remainder of the setup.

This new setup is based on the same principles as the NPC and reaches the same nucleation rates. The main difference is that the OPC consists of two volumes, the measuring volume and the expansion volume, which are separated by a movable piston (see Fig. 1). Again, the main volume is filled with a vapor-carrier gas mixture with the pressure p_0 while the expansion volume is set to a lower pressure. For one measurement, we open the connection between the measuring volume and the expansion volume by moving the piston forward. The mixture expands and nucleation occurs. While the piston moves further forward it closes the connection again. Simultaneously, it recompresses the gas mixture in the main volume by about 5%. This way nucleation and growth are decoupled as well. The detection setup and the evaluation is analogous to the one used in the NPC. The advantage of the OPC over the NPC is the absence of the membrane to provide the recompression. This membrane can be a weak point of the system through possible deformations of the membrane.

III. RESULTS AND DISCUSSION

A. Nucleation rates and comparison with theory

Figure 2 shows the experimental nucleation rates J as a function of supersaturation S. Most experiments were performed in the NPC using argon as carrier gas. In the case of 1-butanol some measurements were also conducted in the OPC (Fig. 2, gray-filled squares). The agreement of results for 1–butanol taken with the OPC and the NPC (white-filled squares) is rather good. Nucleation rates are very sensitive to any deviations or imperfections in the experimental setup or procedure. Therefore, Figure 2 shows quite impressively that creating a nucleation pulse with either chamber leads to consistent and reliable results without apparent systematic errors. For 1–pentanol the measurements with argon (white-filled diamonds) and helium (gray-filled diamonds) as carrier gas also show good agreement, which is well in line with a recent
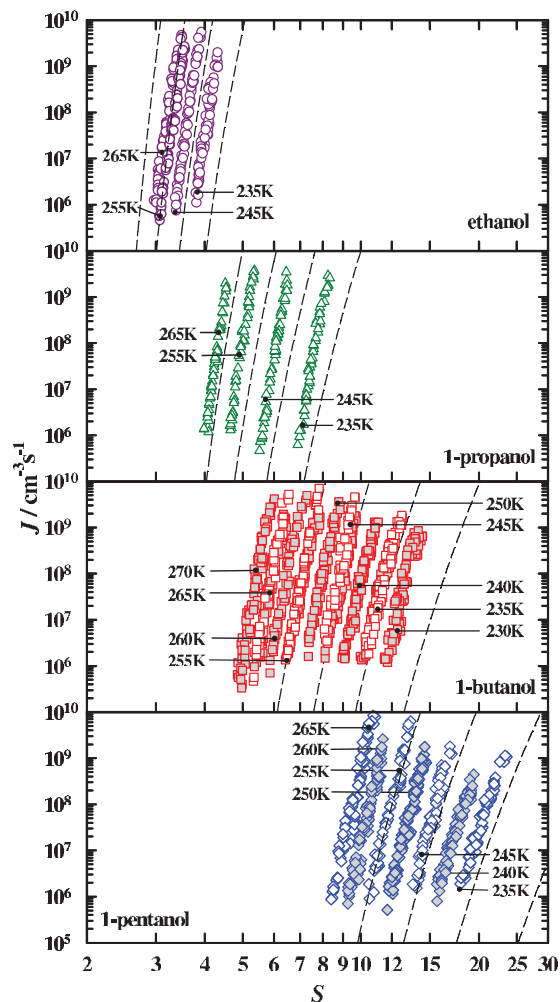
FIG. 2. Isothermal nucleation rates J for ethanol, 1–propanol, 1–butanol, and 1–pentanol[13] as a function of supersaturation S at nucleation temperatures T_{exp} from 235 K to 265 K. Gray-filled squares for 1–butanol represent measurements taken with the one-piston chamber, white-filled squares with the two-valve chamber. Gray-filled diamonds for 1–pentanol are results obtained using helium as carrier gas, instead of argon. Dashed lines represent the predictions by classic nucleation theory at 235 K, 245 K, 255 K, and 265 K for each alcohol, respectively.

description of the influence of the carrier gas on nucleation.[54] The complete results of 1–pentanol are discussed in detail in Ref. 13. Here we included them to compare the nucleation behavior along the homologous series of 1–alcohols more comprehensively.

The nucleation rate isotherms (Fig. 2) shift to higher supersaturations with increasing alcohol chain length. This shift is due to the change in the equilibrium vapor pressure of the 1–alcohols: the equilibrium vapor pressure drops very quickly with increasing chain length, leading to a systematic increase in the supersaturation. The nucleation rate isotherms of ethanol (hexagons) show an atypical behavior: the two isotherms at the highest temperatures (265 K and 255 K) nearly coincide. This effect has already been noticed and investigated by Katz *et al.*[55] and Strey *et al.*[56,57] and is due to the high level of association in the vapor phase at higher vapor pressures and higher temperatures. The influence of this vapor association on nucleation may be explained in two ways.[55–57]

A first intuition might tell us that associated vapors nucleate faster due to the change in the kinetic process because of the more frequent addition of dimers or higher n-mers on route to forming a nucleus. On the other hand, as oligomers form, the number density of monomers decreases and, thus, the overall vapor pressure p_v. This, in turn, severely reduces the supersaturation of the vapor and higher supersaturations are needed to induce or increase nucleation. It turns out that the former kinetic effect is negligible compared to the latter thermodynamic one.[55] Strey *et al.* offered another explanation that takes the release of latent heat during cluster formation in associated vapors into account and also leads to smaller nucleation rates at higher nucleation temperatures. This effect amplifies with increasing nucleation temperature as the amount of condensable and, therefore, also the latent heat release increases.[56,57] Unfortunately, the present data do not lend itself to discriminate one explanation against the other. In fact, it is also possible that both effects play a role and more systematic studies of just ethanol as well as methanol are needed in the future.

The experimental data of all measurements of ethanol, 1–propanol, and 1–butanol,[58] as well as the 1–pentanol data are available online.[13] The thermo-physical data for all alcohols were taken from Schmeling and Strey,[27] Strey and Schmeling,[28] and Frenkel *et al.*[29]

The theoretical predictions are calculated via

$$J_{\text{theory}} = K \exp\left(\frac{-\Delta G^*_{\text{theory}}}{k_B T}\right) \qquad (3)$$

with

$$K = \sqrt{\frac{2\sigma}{\pi m}} \, v_l N_1^2, \qquad (4)$$

and for CNT

$$\Delta G^*_{\text{CNT}} = \frac{16\pi}{3} \frac{v_l^2 \sigma^3}{(kT \ln S)^2}. \qquad (5)$$

Here, K is the kinetic prefactor and ΔG^*_{CNT} is the Gibbs free energy of the formation of a critical cluster according to classical nucleation theory, k is the *Boltzmann* constant, T is the temperature, σ is the planar surface tension, m is the molecular mass, v_l is the volume of one liquid molecule (calculated from the liquid density ρ), and N_1 is the monomer number concentration calculated from the vapor pressure and the ideal gas law. The dashed lines in Figure 2 represent these predictions for the given alcohol and temperatures of 265, 255, 245, and 235 K, respectively.

The *Reguera-Reiss* theory[19,20] (RRT) uses the same "ingredients" in terms of thermophysical properties and the same *Boltzmann*-approach (Eq. (3)) but differs significantly in the cluster definition.[21] In CNT, the cluster is defined as capillary liquid drop of n molecules with radius r. In contrast, the RRT-cluster is defined as a spherical container of radius R and temperature T, enclosing a total number of particles N, which are divided in one capillary (CNT-like) liquid drop of n molecules and $N-n$ surrounding vapor molecules. Among the myriad of possible configurations, *Reguera* and *Reiss* identified the one RRT cluster that corresponds *as a whole* to the critical cluster in an open constant pressure-temperature system, which is
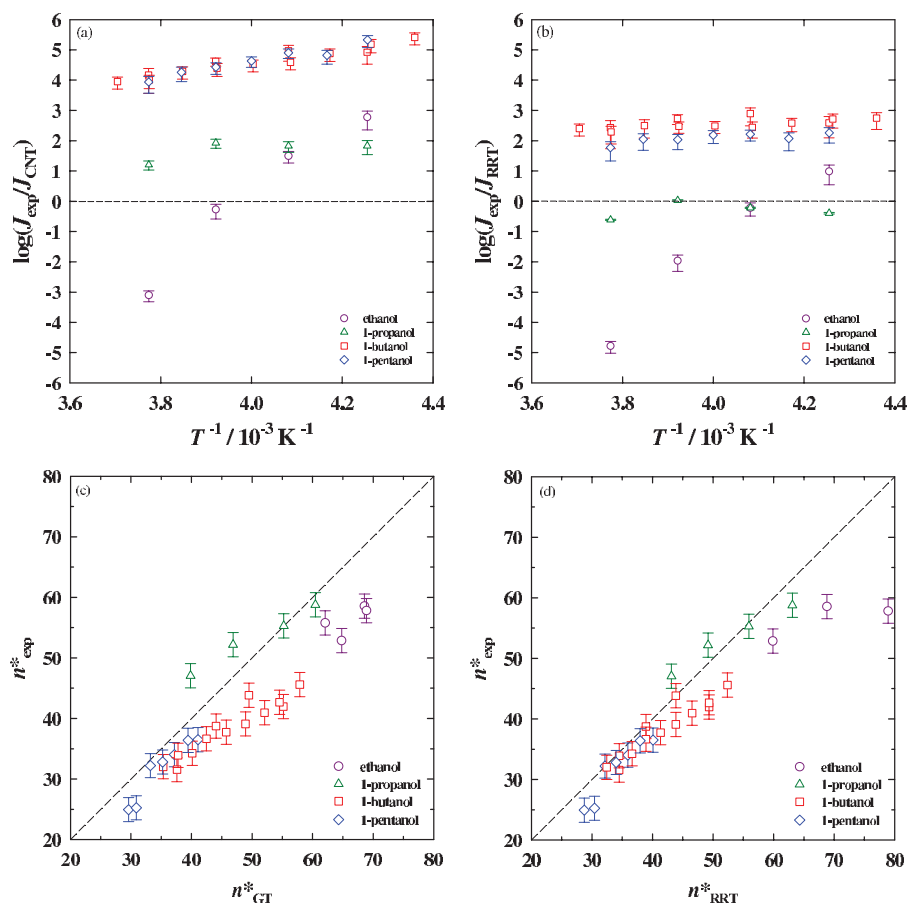
FIG. 3. (a)-(d) Logarithm of the mean value of the ratio of experimental nucleation rates and nucleation rate predictions by CNT J_{exp}/J_{CNT} (left, (a)) and RRT J_{exp}/J_{RRT} (right, (b)) as a function of the inverse temperature T. The dashed line denotes perfect agreement between experiment and theory. (c) The experimentally determined critical cluster sizes n^*_{exp} versus the critical cluster sizes according to *Gibbs-Thomson* n^*_{GT}. The dashed line indicates perfect agreement. (d) Same as (c) for RRT.

precisely the system with a minimum in the total pressure of the RRT cluster. The critical *Gibbs* free energy of formation ΔG^*_{PRT} changes and is then given by

$$\Delta G^*_{RRT} = \Delta F - V_{min}(p_v - P) + N\Delta\mu_0. \quad (6)$$

In this equation, ΔF is the total *Helmholtz* free energy of the cluster, V_{min} is the volume corresponding to a minimum total pressure of the RRT cluster, P is the average total pressure, and $\Delta\mu_0$ is the difference in the chemical potentials $\Delta\mu_0 = kT \ln(p_v / P)$.

For simplicity, we used the same kinetic prefactor K and assumption of perfect vapors (as in CNT) also in the RRT calculations.

In Figure 3, the ratios J_{exp}/J_{CNT} (a) and J_{exp}/J_{RRT} (b) of the experimental nucleation rates and nucleation rates predicted by CNT or RRT, averaged for each nucleation temperature, are plotted as a function of the respective inverse temperature. The dashed horizontal lines represent perfect agreement between experiment and theory.

For 1–butanol (red squares) and 1–pentanol (blue diamonds), CNT underestimates the nucleation rate by 4-5 orders of magnitude, and the deviations increase with decreasing temperature. The comparison with RRT for these substances shows practically constant deviations of about two orders of magnitude with no significant temperature dependence. These

deviations may be due to the CNT prefactor used. Calculations of RRT with other prefactors of Zandi *et al.*[59] show a better agreement with experimental results for 1-pentanol with deviations of less than one order of magnitude over the whole temperature range.

For 1–propanol (green triangles), the predictions of CNT underestimate the rate by 1-2 orders of magnitude with a slight increase with decreasing temperature. In contrast, here the predictions of RRT show astonishingly good agreement with experimental results over the whole temperature range with deviations less than one order of magnitude.

For ethanol (purple circles), both theories fail by several orders of magnitude. CNT predicts too high nucleation rates at temperatures above 250 K, and too low rates below this temperature. At about 255 K, there seem to be perfect agreement. A similar trend is also found for the comparison with RRT. The main difference between the predictions of these theories is that RRT predictions are higher by 2-3 orders of magnitude than CNT predictions and therefore, the temperature of agreement shifts to 245 K.

CNT typically gives agreement at one nucleation temperature for each substance, as already shown by many groups for the alcohols[30,38,41,60] and by Wölk *et al.*,[61] Mikheev *et al.*,[9] and Manka *et al.*[62] for water. Below this temperature, CNT predictions are too low, and above too high. In contrast,

RRT does not show any temperature trend for 1–propanol, 1–pentanol, and 1–butanol and predicts the nucleation rates for all three alcohols quite well. However, for ethanol both theories fail by some orders of magnitude and show strong temperature dependences. As mentioned above, the spontaneous association of molecules in the vapor phase plays a significant role in the nucleation process of ethanol, which makes it difficult to compare it to the other 1–alcohols and unmodified theories. Nevertheless, the lower temperature isotherms of ethanol, with rather low total vapor pressures, where such an effect is smaller, fit quite well into the overall series of alcohols and the comparison with theory.

B. Critical cluster sizes

We determined the excess number of molecules in the critical cluster n_{exp}^* by use of the nucleation theorem[50] in the form

$$n_{exp}^* \approx \left(\frac{\partial \ln J}{\partial \ln S} \right)_T . \tag{7}$$

We made simple straight line fits to the J vs. S isotherms and the critical size thus effectively is an average over the isotherm and mildly neglects its curvature. Assuming a spherical and incompressible cluster as in CNT, we also determined the "critical radii" via

$$r^* = \left(\frac{3 v_l n_{exp}^*}{4\pi} \right)^{\frac{1}{3}} . \tag{8}$$

The results for the critical cluster sizes n_{exp}^* as well as the results for the critical radii r^* as a function of temperature are shown in Figures 4(a) and 4(b), respectively.

The critical cluster sizes n_{exp}^* of all 1–alcohols increase with increasing temperature, except for ethanol. Since the slopes of the isotherms of ethanol change due to its high degree of association in the vapor phase, the proper values of n_{exp}^* are not truly accessible and the apparent critical cluster sizes change. Regarding the homologous series, the number of molecules in the critical cluster is smaller the longer the chain length of the alcohol. In contrast the critical radii are nearly the same for all 1–alcohols, reaching from ∼1.05 nm at 235 K up to ∼1.15 nm at 265 K, being the largest for 1–propanol (about 0.05 nm bigger). This is in good agreement with nucleation theory, which gives the height of the nucleation barrier as $\Delta G^* = \sigma A(n)/3$, where $A(n)$ is the surface area of an assumed spherical cluster.[63] In other words, for similar barrier heights and similar values of surface tension (like for the alcohols), critical clusters should have the same surface area or, likewise, the same radius. Our results seem to confirm that this is indeed the case, supporting at the same time the consistency of the results generated in the nucleation pulse chambers.

Additionally, we calculated n_{GT}^* for each experimental value of S using the *Gibbs-Thomson* equation

$$n_{GT}^* = \frac{32\pi}{3} \frac{v_l^2 \sigma^3}{(kT \ln S)^3} , \tag{9}$$
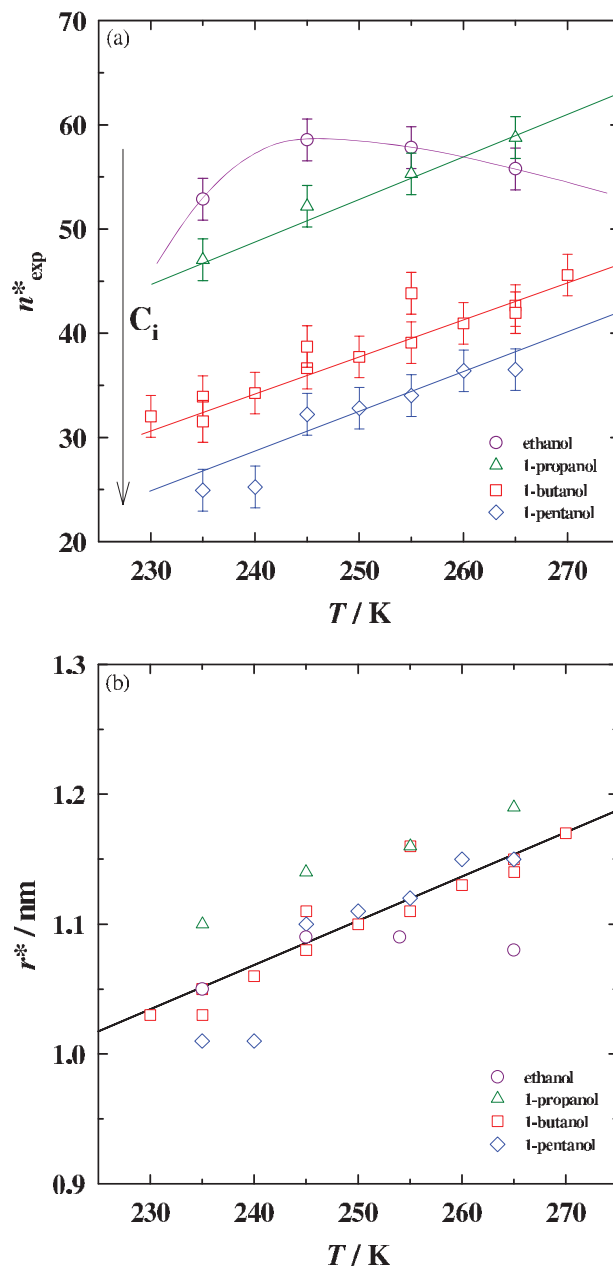
FIG. 4. (a) and (b) The excess number of molecules in a critical cluster n_{exp}^* determined by use of the nucleation theorem (a) and the critical radii r^* (b) of the measured 1–alcohols at the different nucleation temperatures T. The solid lines are just intended to guide the eye.

and averaged over all values corresponding to one nucleation temperature. The comparison between the critical cluster sizes n_{exp}^* and n_{GT}^* is illustrated in Figure 3(c).

The agreement between n_{exp}^* and n_{GT}^* is rather good over the entire range. This demonstrates the importance and accuracy of the first nucleation theorem and underlines the fundamental significance of the *Gibbs-Thomson* relation even for cluster sizes in the nano scale. For 1–butanol and 1–pentanol the *Gibbs-Thomson* predictions agree very well with experimental results at small critical cluster sizes. Surprisingly, the agreement gets worse with increasing cluster size and likewise, increasing temperature (compare to Figure 3(a) but is still quite reasonable. For 1–propanol the *Gibbs-Thomson*

equation predicts slightly too small critical cluster sizes at temperatures about 235–245 K (left side of the ideal line) and at temperatures about 255–265 K the agreement becomes perfect. Hence, a temperature dependence is also observable here. As already mentioned, the values of the experimental critical cluster sizes of ethanol are distorted due to association and no true trend can be observed.

We also determined the critical cluster sizes from the slopes of the Reguera-Reiss isotherms n_{RRT}^* and compared them to n_{exp}^* (Figure 3(d)). Here, the agreement is similar and even better than between n_{exp}^* and n_{GT}^* since all values move together on the line of agreement.

C. Comparison with data from literature

Scaling approaches are a useful way to unify data sets measured with different experimental devices in different temperature and supersaturation regimes. Therefore, we scaled the available data from literature[30–40] with classic nucleation theory (J_{exp}/J_{CNT}) and averaged it over each measuring series at the corresponding nucleation temperature. Figure 5 summarizes the reduced data for ethanol, 1–propanol, and 1–butanol as a function of inverse temperature. The comparison of 1–pentanol can be found in Ref. 13.

The dashed lines in Figure 5 indicate perfect agreement of experiment and theory.

For ethanol, all data sets measured in three different devices; the NPC,[30, 33] the thermal diffusion cloud chamber (TDCC),[31] and the expansion cloud chamber[32] lie together and nearly parallel to each other. We see a consistent picture with linear temperature dependence with CNT over-estimating the nucleation rates above a certain temperature (∼250 K) and underestimating them under this temperature. This is surprising since the measured ethanol nucleation rates did not behave consistently.

For 1-propanol we find a similar temperature trend for all data sets together. Taking a closer look on each measuring series, we can find strong discrepancies from this overall picture. The data measured in the NPC by Strey *et al.*[30] (blue squares) and in the TDCC by Brus *et al.*[35] (yellow squares) show a linear temperature dependence with similar slopes while our data (red circles) and the data measured in a supersonic nozzle (SSN) by Ghosh *et al.*[37] (light blue hexagons) are nearly constant over the entire range. In contrast, Graß-mann and Peters[34] (gray triangles down) found an inverted temperature dependence in a piston-expansion tube and the data by Kacker and Heist[31] (violet triangles up) also measured in a thermal diffusion cloud chamber shows a zig-zag pro-file. These different temperature trends are surprising since the data by Strey *et al.*[30] and our data have been measured with the same experimental technique (NPC) as well as the data by Kacker and Heist[31] and Brus *et al.*[35] are both measured in a TDCC.

The overall picture for 1–butanol is remarkable since the data sets altogether show the above-mentioned temperature trend, but looking at the series of measurement separately, most series display an inverted temperature trend. Our data
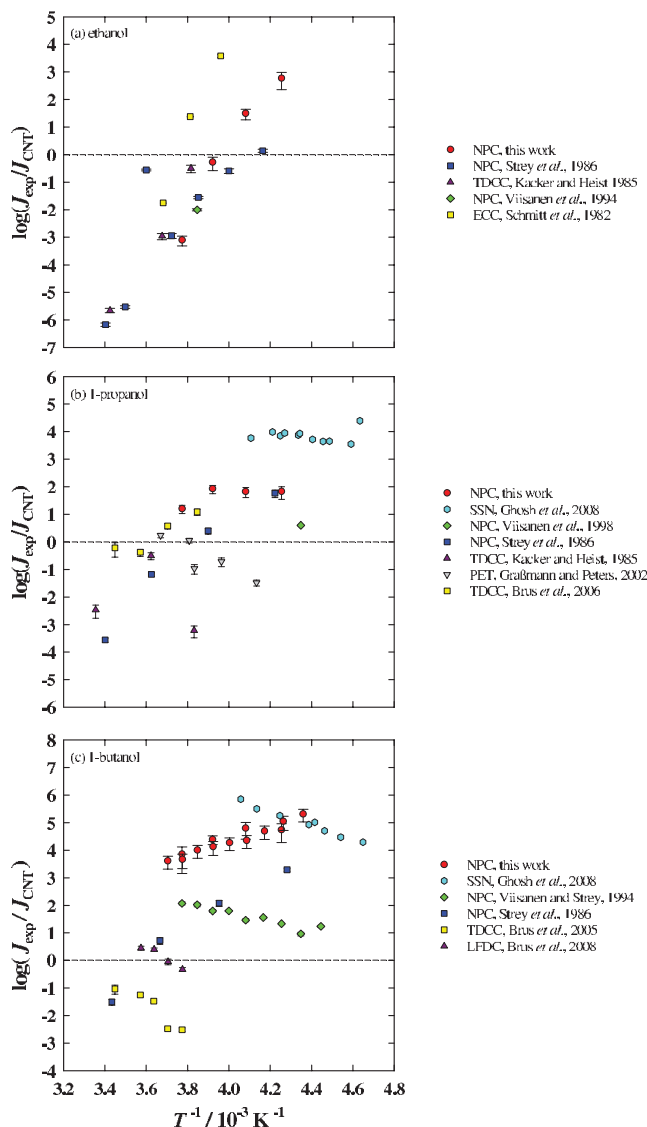
FIG. 5. (a)-(c) Logarithm of the mean values of experimental nucleation rates from literature[30–40] scaled with CNT J_{exp}/J_{CNT} as a function of the inverse temperature T for ethanol (a), 1–propanol (b), and 1–butanol (c). The dashed lines represent perfect agreement between experiment and theory.

(red circles) and the data by Strey *et al.*[30] (blue squares), both measured in the NPC, show the "normal" temperature trend, whereas the slope of the Strey *et al.*[30] data is much steeper. The measurement series by Ghosh *et al.*[37] in the SSN (light blue hexagons), Viisanen and Strey[38] in the NPC (green di-amonds), and Brus *et al.*[39, 40] in the TDCC as well as in a laminar flow diffusion chamber (yellow squares and violet tri-angles, respectively) exhibit the inverted temperature depen-dence. They all lie parallel to each other, separated by 1–4 orders of magnitude. Although our data, the data by Strey *et al.*,[30] and the data by Viisanen and Strey[38] have been mea-sured in the same device, we find different temperature trends for each of these series. To date it is not understood if these de-viations in temperature dependence originate from improve-ments in the setup of the apparatus, which has been updated over the years.

IV. SUMMARY AND CONCLUSION

We measured homogeneous nucleation rates of the 1–alcohols ethanol, 1–propanol, and 1–butanol systematically at temperatures between 235 and 265 K in the two-valve nucleation pulse chamber. For part of the 1–butanol measurements we also used a novel one-piston expansion chamber. Similar results with both techniques show that either method produces reliable and reproducible nucleation rates and that no systematic error is inherent in our system. Moreover, if there were a systematic error, the very consistent results obtained for the homologous series by two different setups (one-piston expansion chamber and the two-valve nucleation pulse chamber) suggest that such an error should be constant for all measurements. Thus, our data represent a comprehensive and reliable data set that is ideal for comparison with nucleation theory. We compared our data, including the 1–pentanol data of Iland *et al.*,[13] with classic nucleation theory[14] and Reguera-Reiss theory.[19,20] For 1–propanol, CNT seems to yield acceptable predictions with deviations about 1-3 orders of magnitude, while RRT is able to predict nucleation rates nearly perfectly. The CNT predictions for 1–butanol and 1–pentanol fail by 3-5 orders of magnitude, increasing with decreasing temperature. Here, the RRT predictions are too small by about two orders of magnitude over all measured nucleation temperatures with no observable temperature trend. This deviation may be related to the used kinetic pre-factor of CNT. By extrapolating the nucleation rate comparison with CNT to other temperatures the same trend could be observed for all alcohols: there is one temperature for each alcohol where CNT predictions and experimental results coincide, underneath this temperature the theoretical predictions are too low, above, they are too high. This temperature trend is not observed for the nucleation rate predictions by RRT. For ethanol, no theory could provide sufficient predictions underneath and above a defined temperature, respectively, because of its high grade of association in the vapor phase, which is not considered in either theory.

We determined the critical cluster sizes n^*_{exp} and compared them to cluster sizes calculated using the *Gibbs-Thomson* equation n^*_{GT} and Reguera-Reiss theory n^*_{RRT}. The agreement between n^*_{exp} and n^*_{GT} is rather good at small cluster sizes, with increasing cluster size it becomes worse but is still quite reasonable. The comparison between n^*_{exp} and n^*_{RRT} shows the same behavior but the agreement is even better.

To compare our data to literature data[30–40] we scaled it with classic nucleation theory. For ethanol, one temperature trend for all measurement series can be found. For 1–propanol, 1–butanol, and 1–pentanol[13] the overall picture also shows this temperature trend, but taking a closer look on the individual measurement series, significant differences from this temperature trend can be found. Overall, no other data apart from the nucleation pulse chamber appear to yield a consistent trend across the homologous series.

[1] C. R. T. Wilson, Philos. Trans. R. Soc. London, Ser. A **189**, 265 (1897).
[2] R. H. Heist and H. J. He, J. Phys. Ref. Data **23**, 781 (1994).
[3] P. P. Wegener, in *Gas Dynamics*, edited by P. P. Wegener (Marcel Dekker, New York, 1966).
[4] B. E. Wyslouzil, G. Wilemski, M. G. Beals, and M. B. Frish, Phys. Fluids **6**(8), 2845–2854 (1994).
[5] F. Peters, Exp. Fluids **1**, 143–148 (1983).
[6] J. L. Katz and B. J. Ostermier, J. Chem. Phys. **47**(2), 478 (1967).
[7] R. H. Heist, M. Janjua, and J. Ahmed, J. Chem. Phys. **98**(16), 4443–4453 (1994).
[8] J. Smolík and V. Ždímal, Aerosol Sci. Technol. **20**, 127 (1994).
[9] V. B. Mikheev, P. M. Irving, N. S. Laulainen, S. E. Barlow, and V. V. Pervukhin, J. Chem. Phys. **116**(24), 10772–10786 (2002).
[10] H. Lihavainen and Y. Viisanen, J. Phys. Chem. B **105**, 11619 (2001).
[11] P. E. Wagner and R. Strey, J. Phys. Chem. **85**(18), 2694–2698 (1981).
[12] R. Strey, P. E. Wagner, and Y. Viisanen, J. Phys. Chem. **98**(32), 7748–7758 (1994).
[13] K. Iland, J. Wedekind, J. Wölk, P. E. Wagner, and R. Strey, J. Chem. Phys. **121**(24), 12259 (2004).
[14] R. Becker and W. Döring, Ann. Phys. (Leipzig) **24**, 719 (1935).
[15] L. Farkas, Z. Phys. Chem. (Leipzig) **125**, 236 (1927); online at http://www.physik.uni-augsburg.de/theo1/hanggi/History/Farkas.pdf.
[16] M. Volmer and A. Weber, Z. Phys. Chem. (Leipzig) **119**, 227 (1926).
[17] D. W. Oxtoby and R. Evans, J. Chem. Phys. **89**(12), 7521 (1988).
[18] G. K. Schenter, S. M. Kathmann, and B. C. Garret, Phys. Rev. Lett. **82**(17), 3484 (1999).
[19] D. Reguera and H. Reiss, Phys. Rev. Lett. **93**(16), 165701 (2004).
[20] D. Reguera and H. Reiss, J. Phys. Chem. B **108**(51), 19831 (2004).
[21] D. Reguera, R. K. Bowles, Y. S. Djikaev, and H. Reiss, J. Chem. Phys. **118**(1), 340 (2003).
[22] D. Reguera and H. Reiss, J. Chem. Phys. **119**(3), 1533–1546 (2003).
[23] V. I. Kalikmanov, J. Chem. Phys. **124**(12), 124505 (2006).
[24] B. Nowakowski and E. Ruckenstein, J. Chem. Phys. **94**(2), 1397 (1991).
[25] D. Kashchiev, J. Chem. Phys. **118**(4), 1837 (2003).
[26] K. Iland, J. Wölk, R. Strey, and D. Kashchiev, J. Chem. Phys. **127**, 154506 (2007).
[27] T. Schmeling and R. Strey, Ber. Bunsenges. Phys. Chem. **87**, 871 (1983).
[28] R. Strey and T. Schmeling, Ber. Bunsenges. Phys. Chem. **87**, 324 (1983).
[29] M. Frenkel, X. Hong, R. C. Wilhoit, and K. R. Hall, *Landolt-Börnstein Group IV - Physical Chemistry* (Springer-Verlag, Heidelberg, 2000).
[30] R. Strey, P. E. Wagner, and T. Schmeling, J. Chem. Phys. **84**(4), 2325 (1986).
[31] A. Kacker and R. H. Heist, J. Chem. Phys. **82**(6), 2734–2744 (1985).
[32] J. L. Schmitt, G. W. Adams, and R. A. Zalabsky, J. Chem. Phys. **77**(4), 2089 (1982).
[33] Y. Viisanen, R. Strey, A. Laaksonen, and M. Kulmala, J. Chem. Phys. **100**(8), 6062–6072 (1994).
[34] A. Graßmann and F. Peters, J. Chem. Phys. **116**(17), 7617–7620 (2002).
[35] D. Brus, V. Ždímal, and F. Stratmann, J. Chem. Phys. **124**(16), 164306 (2006).
[36] Y. Viisanen, P. E. Wagner, and R. Strey, J. Chem. Phys. **108**(10), 4257–4266 (1998).
[37] D. Ghosh, A. Manka, R. Strey, S. Seifert, R. E. Winans, and B. E. Wyslouzil, J. Chem. Phys. **129**, 124302 (2008).
[38] Y. Viisanen and R. Strey, J. Chem. Phys. **101**(9), 7835–7843 (1994).
[39] D. Brus, A.-P. Hyvärinen, V. Ždímal, and H. Lihavainen, J. Chem. Phys. **122**, 214506 (2005).
[40] D. Brus, A.-P. Hyvärinen, V. Ždímal, and H. Lihavainen, J. Chem. Phys. **128**, 079901 (2008).
[41] M. M. Rudek, J. L. Katz, I. V. Vidensky, V. Ždímal, and J. Smolík, J. Chem. Phys. **111**(8), 3623 (1999).
[42] C. C. M. Luijten, O. D. E. Baas, and M. E. H. van Dongen, J. Chem. Phys. **106**(10), 4152 (1997).
[43] V. Ždímal and J. Smolík, Atmos. Res. **46**, 391 (1998).
[44] A. Graßmann and F. Peters, J. Chem. Phys. **113**(16), 6774–6781 (2000).
[45] R. Strey, Y. Viisanen, and P. E. Wagner, J. Chem. Phys. **103**(10), 4333–4345 (1995).
[46] J. Hrubý, Y. Viisanen, and R. Strey, J. Chem. Phys. **104**(13), 5181–5187 (1996).

[47]H. Lihavainen, Y. Viisanen, and M. Kulmala, J. Chem. Phys. **114**(22), 10031 (2001).

[48]H. Lihavainen, Y. Viisanen, and M. Kulmala, J. Chem. Phys. **128**(13), 139902 (2008).

[49]J. L. Schmitt and G. J. Doster, J. Chem. Phys. **116**(5), 1976–1978 (2002).

[50]D. Kashchiev, J. Chem. Phys. **76**(10), 5098 (1982).

[51]D. W. Oxtoby and D. Kashchiev, J. Chem. Phys. **100**, 7665 (1994).

[52]R. K. Bowles, R. McGraw, P. Schaaf, B. Senger, J.-C. Voegel, and H. Reiss, J. Chem. Phys. **113**(11), 4524–4532 (2000).

[53]P. E. Wagner, J. Colloid Interface Sci. **105**, 456 (1985).

[54]J. Wedekind, A.-P. Hyvärinen, D. Brus, and D. Reguera, Phys. Rev. Lett. **101**(12), 125703 (2008).

[55]J. L. Katz, H. Saltsburg, and H. Reiss, J. Colloid Interface Sci. **21**, 560–568 (1966).

[56]R. Strey, T. Schmeling, and P. E. Wagner, J. Chem. Phys. **85**(10), 6192–6196 (1986).

[57]R. Strey, T. Schmeling, and P. E. Wagner, J. Aerosol Sci. **17**(3), 459–461 (1986).

[58]See supplementary material at http://dx.doi.org/10.1063/1.4739096 for the complete data of the measurements for 1-pentanol.

[59]R. Zandi, D. Reguera, and H. Reiss, J. Phys. Chem. B **110**, 22251 (2006).

[60]D. Brus, A. P. Hyvärinen, J. Wedekind, Y. Viisanen, M. Kulmala, V. Ždímal, J. Smolík, and H. Lihavainen, J. Chem. Phys. **128**(13), 134312 (2008).

[61]J. Wölk, R. Strey, C. H. Heath, and B. E. Wyslouzil, J. Chem. Phys. **117**(10), 4954–4960 (2002).

[62]A. A. Manka, D. Brus, A. P. Hyvarinen, H. Lihavainen, J. Wölk, and R. Strey, J. Chem. Phys. **132**, 244505 (2010).

[63]F. F. Abraham, *Homogeneous Nucleation Theory: The Pretransition Theory of Vapor Condensation* (Academic, New York, 1974).